Organic Electronics 10 (2009) 562–567

Contents lists available at ScienceDirect

Organic Electronics

journal homepage: www.elsevier.com/locate/orgel

# Influence of side chain symmetry on the performance of poly(2,5-dialkoxy-*p*-phenylenevinylene): fullerene blend solar cells

Sachetan M. Tuladhar [a,*], Marc Sims [a,b], Stelios A. Choulis [a,c], Christian B. Nielsen [d], Wayne. N. George [d], Joachim H.G. Steinke [d], Donal D.C. Bradley [a], Jenny Nelson [a,*]

[a] Department of Physics, Imperial College London, Prince Consort Road, London SW7 2AZ, UK
[b] DuPont Displays Inc., 6780 Cortona Drive, Santa Barbara, California 93101, USA
[c] Department of Mechanical Engineering and Materials Science and Engineering, Cyprus University of Technology, 3603 Limassol, Cyprus
[d] Department of Chemistry, Imperial College London, London SW7 2AY, UK

ARTICLE INFO

*Article history:*
Received 14 October 2008
Received in revised form 6 February 2009
Accepted 9 February 2009
Available online 20 February 2009

*Keywords:*
DialkoxyPPV
Fullerene
Side chain symmetry
Bulk heterojunction
Organic photovoltaic
Cells
Charge transport

ABSTRACT

We report on studies of poly-(2,5-dihexyloxy-*p*-phenylenevinylene) (PDHeOPV), a symmetric side-chain polymer, as a potential new donor material for polymer:fullerene blend solar cells. We study the surface morphology of blend films of PDHeOPV with PCBM, the transport properties of the blend films, and the performance of photovoltaic devices made from such blend films, all as a function of PCBM content. In each case, results are compared with those obtained using the asymmetric side chain polymer, poly[2-methoxy-5-(3,7-dimethyloctyloxy)-1,4-phenylenevinylene] (MDMO-PPV), in order to investigate the influence of polymer side chain symmetry on solar cell performance. AFM images show that large PCBM aggregates appear at lower PCBM content (50 wt.% PCBM) for PDHeOPV:PCBM than for MDMO-PPV:PCBM (67 wt.% PCBM) blend films. Time-of-Flight (ToF) mobility measurements show that charge mobilities depend more weakly on PCBM content in PDHeOPV:PCBM than in MDMO:PPV:PCBM, with the result that at high PCBM content the mobilities in PDHeOPV:PCBM are significantly lower than in MDMO:PPV:PCBM blend films, despite the higher mobilities in pristine PDHeOPV compared to pristine MDMO-PPV. Photovoltaic devices show significantly lower power conversion efficiency (~0.93%) for PDHeOPV:PCBM (80 wt.% PCBM) blend films than for MDMO-PPV:PCBM (2.2% at 80 wt.% PCBM) blends. This is attributed to the relatively poor transport properties of the PDHeOPV:PCBM blend, which limit the optimum thickness of the photoactive layer in PDHeOPV:PCBM blend devices. The behaviour is tentatively attributed to a higher tendency for the symmetric side-chain polymer chains to aggregate, resulting in poorer interaction with the fullerene and poorer network formation for charge transport.



## 1. Introduction

The performance of bulk heterojunction solar cells based on the blend of a conjugated polymer and a fullerene derivative is critically dependent on the nano- and micro-scale morphology of the thin solution-processed semiconductor blend layer [1–6]. In several systems it has been observed that optimum device performance is achieved for blend films that feature a certain degree of phase separation (~10 nm length scale). This positive effect of phase segregation is attributed to improved charge transport or light harvesting as a result of increased crystallinity of components [7] and to a reduction in bimolecular [8] or geminate [9] charge recombination with less intimate phase mixing. Large scale (>100 nm) phase segregation, on the other hand, leads to poor device performance due to the limited interfacial area available for charge

* Corresponding authors. Tel.: +4402075946679 (S.M. Tuladhar); tel.: +4402075947581 (J. Nelson).
*E-mail addresses:* s.tuladhar@imperial.ac.uk (S.M. Tuladhar), nelson@imperial.ac.uk (J. Nelson).

1566-1199/$ - see front matter © 2009 Elsevier B.V. All rights reserved.
doi:10.1016/j.orgel.2009.02.008

separation [10]. Control of the microstructure of the active layer is therefore critical for the optimisation of photovoltaic device performance.

One means by which the blend morphology can be controlled is through the self-organising nature of the molecular components used, for instance, the degree of crystallinity of the polymer or fullerene [7] or the interaction energy between the components [11]. In the case of conjugated polymers, polymer chain packing is known to be influenced by the length and nature of the polymer side chains. In particular, symmetric side chains in poly-*p*-phenylenevinylene (PPV) polymers are known to lead to more rigid chain conformations and a higher degree of chain aggregation than asymmetric chains [12,13]. A recent study by Blom and co-workers [14,15] has shown that hole transport in blend films of a symmetrically substituted PPV polymer with PCBM is insensitive to composition, in contrast to blend films of the widely studied asymmetrically substituted polymer poly[2-methoxy-5-(3',7'-dimethyloctyloxy)-1-4-phenylene vinylene] (MDMO-PPV) with PCBM, suggesting that side chain symmetry can affect blend film morphology. In this paper, we investigate the influence of the polymer donor side chain symmetry on the morphology of PPV polymer:PCBM blend films, on charge transport in the blend films and on the behaviour of the corresponding bulk heterojunction photovoltaic devices. We select two alternative dialkoxy-*p*-phenylenevinylene polymers as the donor material, the symmetrically substituted polymer 2,5-dihexyloxy-*p*-phenylenevinylene (PDHeOPV) and the asymmetrically substituted polymer MDMO-PPV. We show that the symmetrically substituted polymer leads to larger scale phase separation and poorer device performance, and that the differences in device performance are correlated both to the different degree of phase segregation and to a very different dependence of the electron and hole transport properties of the blend films on PCBM content. The results demonstrate the critical influence of polymer phase behaviour on bulk heterojunction performance.

## 2. Experimental

The PDHeOPV polymer (number average molecular weight ~25 kDa (approximately 82 repeat units)) was prepared as detailed in Ref. [16]. For atomic force microscopy (AFM, Burleigh Instruments) and photoluminescence (PL, FluoroMax-3, Jobin-Yvon) measurements, blend films of thickness ~50 nm were spin coated from chlorobenzene solution onto indium tin oxide (ITO) coated glass substrates coated with a ~70 nm layer of polystyrene sulphonate doped poly(ethylenedioxythiophene) (PEDOT:PSS). This sample structure was used in order to simulate conditions in the solar cell as closely as possible, since it is known that substrate influences phase segregation. Devices for time-of-flight (ToF) mobility measurements were made by spin coating films of pristine PDHeOPV and blend films of PDHeOPV:PCBM blends containing 0, 20, 33, 50, 67 and 75 wt.% PCBM from chlorobenzene solutions onto indium tin oxide (ITO) coated glass substrates. Pristine films of PDHeOPV (92 mg/ml) and blend films of PDHeOPV:PCBM containing 20 (18 mg/ml), 33 (30 mg/ml), 50 (45 mg/ml), 67 (60 mg/ml) and 75 (67 mg/ml) wt.% PCBM were spin-coated on to ITO at spin speeds of 2000, 1800, 1500, 1500 and 1000 rpm, respectively. The ToF devices were then completed by thermal evaporation of a shadow masked, aluminum top contact (~100 nm), at a typical pressure of $10^{-6}$ mbar. Film thicknesses were measured with a Sloan Dektak™ surface profilometer. Hole mobility values were obtained by analysis of ToF photocurrent transients as described in Ref. [17]. Bulk heterojunction solar cells with the sandwich structure ITO/PEDOT:PSS (70–75 nm)/X/Al were fabricated where X was a blend layer of either PDHeOPV or MDMO-PPV with a varying weight fraction of PCBM. All devices were illuminated through the semitransparent ITO electrode with AM1.5G light from a filtered Xe lamp at an intensity of 100 mW/cm$^2$.

## 3. Results and discussions

The electric field dependence of hole mobility of PDHeOPV and MDMO-PPV at room temperature is shown in Fig. 1. The data for both samples follow the Poole-Frenkel form, generally found in a wide range of disordered materials [18]. The hole mobility of symmetrically substituted PDHeOPV (~$10^{-5}$ cm$^2$/Vs) at low fields is about an order of magnitude higher than the hole mobility of the asymmetrically substituted MDMO-PPV (~$10^{-6}$ cm$^2$/Vs). This is also true of the hole mobility of other symmetrically substituted dialkoxy-poly-*p*-phenylene vinylenes, even those with longer side chains [16]. The higher low field mobility for the symmetrically than for the asymmetrically substituted PPVs thus implies that the nature of chain packing is important in determining the hole-transporting characteristics of these materials. This is reflected in the ToF photocurrent transients shown in the inset to Fig. 1. The photocurrent transients of PDHeOPV films exhibit relatively non-dispersive behaviour (characterised by the pronounced knee in the transient when plotted on double logarithmic axes) in comparison to MDMO-PPV at similar fields. Weak dependence of hole mobility on electric field, such as that seen for PDHeOPV in Fig. 1, is often correlated with low energetic disorder and non-dispersive charge transport [19].

Fig. 2 shows the zero-field electron and hole mobilities in PDHeOPV:PCBM blend films as a function of PCBM content, obtained by extrapolation of Poole-Frenkel fits to the field dependent mobility data. The zero-field ToF mobility of holes and electrons in MDMO-PPV:PCBM blend films [20] are also presented as a function of PCBM content in the same plot for comparison. Whilst both electron and hole mobility increase continuously with increasing PCBM content from 16 to 67 wt.% PCBM in the case of MDMO-PPV:PCBM blend films, leading to a net increase of two to four orders of magnitude, the zero-field electron and hole mobilities of PDHeOPV:PCBM blends are relatively insensitive to PCBM content. The mild increase in electron mobility with PCBM content in PDHeOPV:PCBM blends can be attributed to improved electron percolation with PCBM network formation. A similar weak dependence of hole mobility on PCBM content was observed previously for an-

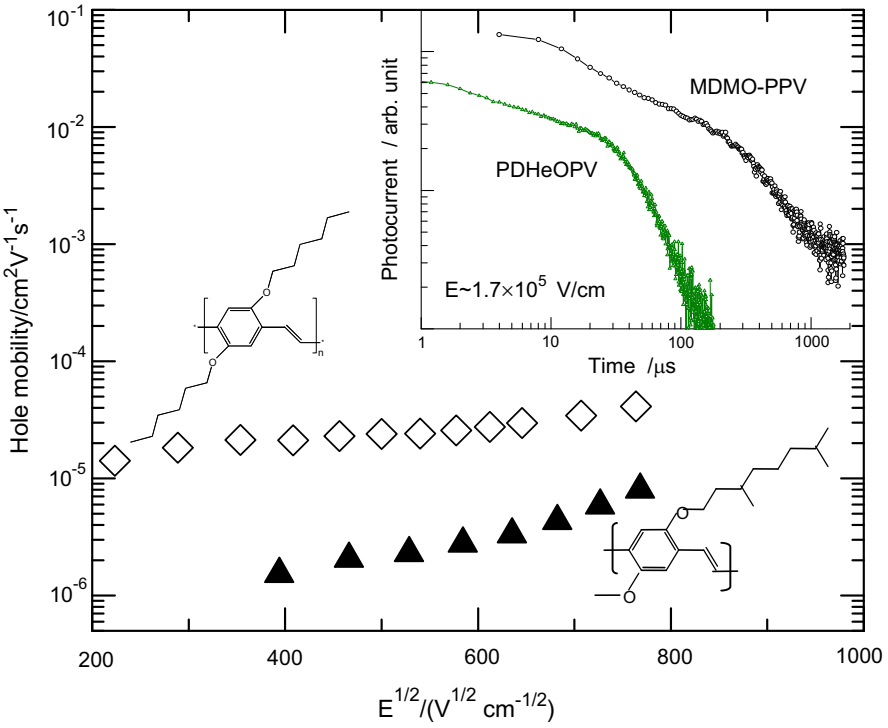


**Fig. 1.** The electric field dependent ToF hole mobility at room temperature in pristine PDHeOPV (open diamonds) and MDMO-PPV (filled triangles) films of thicknesses 1.2 and 1.6 μm, respectively. The inset shows the structure of the respective polymers and the ToF photocurrent transients for PDHeOPV, MDMO-PPV samples plotted on double logarithmic axes at similar electric field $\sim 1.7 \times 10^5$ V/cm.

other symmetrically substituted dialkoxy PPV polymer [14]. Although the strong dependence of charge transport on PCBM content observed for MDMO-PPV:PCBM blend films has not been unambiguously explained, the influence of PCBM on polymer chain packing is thought to be relevant [6,20].

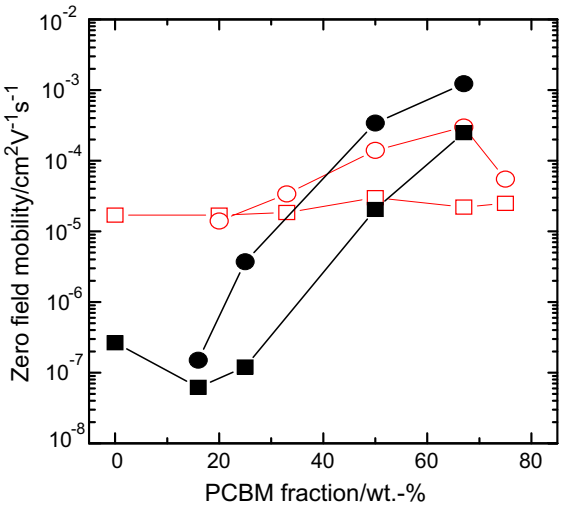


**Fig. 2.** Zero-field electron (circles) and hole mobilities (squares) in (a) PDHeOPV:PCBM and (b) MDMO-PPV: PCBM blends as a function of PCBM concentration. Open symbols represent PDHeOPV:PCBM and filled symbols MDMO-PPV:PCBM blends.

The very different composition dependence of charge carrier mobilities in PDHeOPV:PCBM blends compared to MDMO-PPV:PCBM may result from different polymer chain conformations. Symmetric side chain polymers are expected to assume more rigid conformations [12] and therefore the PDHeOPV chain morphology may be less strongly affected by the presence of PCBM than MDMO-PPV with its asymmetric side chains and tendency to form ring-like structures [13]. This difference may be enhanced by the fact that the side chains in MDMO-PPV are branched while those in PDHeOPV are linear. The observation of phase segregation at 50 wt.% PCBM in PDHeOPV:PCBM blends while none is seen in MDMO-PPV:PCBM until ~67 wt.% [3,21] is consistent with the hypothesis that the more rigid, symmetrically substituted PDHeOPV polymer chains have a stronger tendency to aggregate than the asymmetrically substituted MDMO-PPV chains, and consequently are less strongly affected by the presence of PCBM.

Fig. 3 shows the photoluminescence spectra (480 nm excitation) for PDHeOPV:PCBM blend films as a function of PCBM content. The PL of PDHeOPV is increasingly quenched with the addition of PCBM up to a content of 70–80 wt.% PCBM, consistent with photoinduced charge transfer in these composite films. The PL spectra of the PDHeOPV:PCBM blend films exhibit well resolved vibronic structure and resemble the spectra of pristine PDHeOPV [16], at all PCBM contents. In contrast, it has been shown

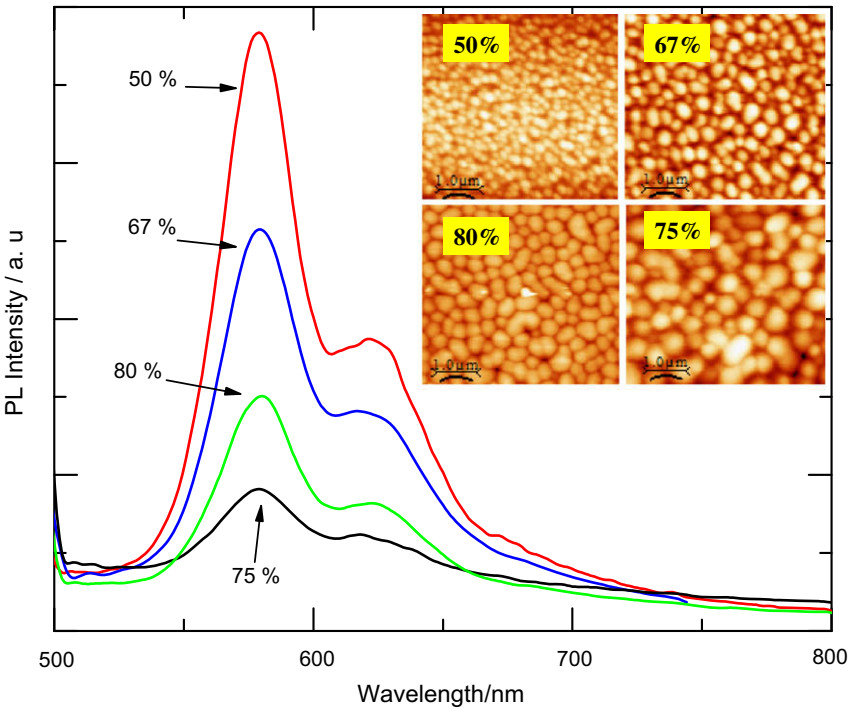


**Fig. 3.** PL spectra from PDHeOPV:PCBM blend films as a function of PCBM weight percentage for excitation at 480 nm. The inset shows the AFM phase images of the PDHeOPV:PCBM blend films of 80, 75, 67 and 50 wt.% PCBM.

that the PL spectra of MDMO-PPV:PCBM blend films become structureless with increasing PCBM content, completely losing the red shoulder seen in the PL spectrum of pristine MDMO-PPV at PCBM contents greater than 30 wt.% [3]. This again suggests that the morphology of the blend film made from the symmetrically substituted polymer will be quite different from that of the blend made from the asymmetrically substituted polymer.

As a further probe of morphology, the PDHeOPV:PCBM blend films were studied with atomic force microscopy (AFM) as a function of PCBM content. Fig. 3 (inset) shows the height images obtained by AFM for composite PDHeOPV:PCBM films (~50 nm) for four different compositions. Whilst the surface roughness of pristine films of both PDHeOPV and PCBM films is low (root-mean-square roughness, $z_{RMS} < 1$ nm), the PDHeOPV:PCBM blend films are rough ($z_{RMS} \geqslant 10$ nm) and exhibit separate domains of diameter >100 nm, with both surface roughness and domain size increasing with PCBM content. These roughness values and domain sizes are much larger than those observed for MDMO-PPV:PCBM blend films at similar PCBM content ($z_{RMS} < 1$ nm, domain size 60–80 nm at 80 wt.% PCBM [3,10] compared to $z_{RMS} \sim 12$ nm, domain size 500 nm for PDHeOPV:PCBM). Larger domains may lead to a lower efficiency of exciton dissociation, depending on the purity of the domains observed. The height fluctuations of the PDHeOPV:PCBM blend films thus account for a significant fraction of the total thickness of the thin films used to make devices, as discussed below.

Photovoltaic devices were made from PDHeOPV:PCBM blends containing 50, 67, 75 and 80 wt.% PCBM. The highest EQE was obtained at 80 wt.% PCBM. To optimise device structure, device performance was then studied as a function of blend film thickness for the composition (80 wt.% PCBM). Film thickness was varied from 50 to 240 nm by changing either solution concentration or the rate of spin coating. For all devices, blend films were spin coated on to PEDOT:PSS layers (70–75 nm thick) and finished with Al top contacts. A similar series of MDMO-PPV:PCBM de-

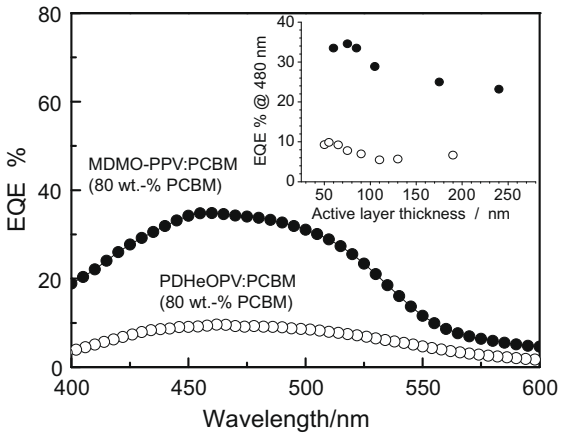


**Fig. 4.** External quantum efficiency (EQE) spectra for PDHeOPV:PCBM (80 wt.% PCBM) and MDMO-PPV:PCBM (80 wt.% PCBM) blend devices with photoactive layer film thicknesses of 55 nm and 75 nm, respectively. The inset shows the EQE of both blends with various photoactive layer thicknesses at an excitation wavelength of 480 nm.

vices was made for comparison and the resulting EQE spectra are depicted in Fig. 4. The data clearly show that the EQE of the devices based on PDHeOPV:PCBM is substantially lower than that of MDMO-PPV:PCBM based devices, across the thicknesses range. The EQE shows a maximum 35% for the MDMO-PPV:PCBM device with a 75 nm thick active layer while for the PDHeOPV:PCBM devices, the lowest thickness studied (50–55 nm) produced the highest EQE (~10%). Good quality devices with thinner active layers could not be made, probably due to defects such as pinholes in the active layer.

The value of the optimum active layer thickness in a bulk heterojunction solar cell is determined by the competition between light absorption and charge carrier mobility. Given that the optical absorption of the two polymers is similar, the lower optimum thickness for PDHeOPV:PCBM than for MDMO-PPV:PCBM is consistent with the lower electron and hole mobilities of the former blend.

Fig. 5 shows a plot of the photovoltaic parameters, the short circuit current density, $J_{sc}$, open circuit voltage, $V_{oc}$, power conversion efficiency $\eta$ and fill factor FF for the series of PDHeOPV:PCBM (80 wt.% PCBM) devices with different active layer thickness in comparison with those for a series of MDMO-PPV:PCBM (80 wt.% PCBM) devices.

The dependence of $J_{sc}$ on active layer thickness for PDHeOPV:PCBM and MDMO-PPV:PCBM blend devices resembles that of the EQE with an optimum at 55 nm for PDHeOPV:PCBM and at 75 nm for MDMO-PPV:PCBM, after which $J_{sc}$ tends to decrease with increasing thickness as a result of the competition between transport and recombination, as discussed above. In the case of MDMO-PPV:PCBM blend devices $J_{sc}$ shows a broad local minimum around ~100 nm which can be attributed to optical interference and is expected theoretically [22]. Similar structure is also visible in the case of PDHeOPV:PCBM blend films.

Open-circuit voltages were comparable for the two blend types (~0.7–0.8 V) and relatively insensitive to film thickness, as previously observed [23,24]. However, a fall-off in both $V_{oc}$ and fill factor with reducing thickness for the thinnest PDHeOPV:PCBM blend devices suggests shunt losses possibly due to non-uniformities in film thickness.

The highest power conversion efficiencies are found for the device thicknesses that led to the highest $J_{sc}$, i.e. 55 nm ($\eta$ = 0.93%) in the case of PDHeOPV:PCBM blend devices and 75 nm ($\eta$ = 2.2%) in the case of MDMO-PPV:PCBM blend devices, in good agreement with previous results for solar cells based on same materials [10]. The inferior performance of PDHeOPV:PCBM devices compared to MDMO-PPV:PBM is likely to result from the lower photon to electron conversion efficiency, resulting both from the lower mobility (enhancing recombination) and the relatively large domain size (possibly reducing exciton dissociation efficiency) relative to MDMO-PPV:PCBM. In addition, the relatively high surface roughness (~10 nm) is likely to limit the performance of thinner devices through charge leakage along shunt paths between the electrodes.

## 4. Conclusions

Polymer:PCBM blend films and devices were made using dialkoxyPPV polymers with symmetric (PDHeOPV) and asymmetric (MDMO-PPV) side chains and their transport and photovoltaic properties were studied. The effects of PCBM content and active layer thickness on PDHeOPV:PCBM blend photovoltaic device parameters were also examined. We have optimised the active layer thickness for PDHeOPV:PCBM and MDMO-PPV:PCBM blend solar cells and found efficiency maxima of 0.93% at 55 nm for PDHeOPV:PCBM and 2.2% at 75 nm for MDMO-PPV:PCBM devices. The maximum EQE for PDHeOPV:PCBM blend devices was found to be about 10% in the range of

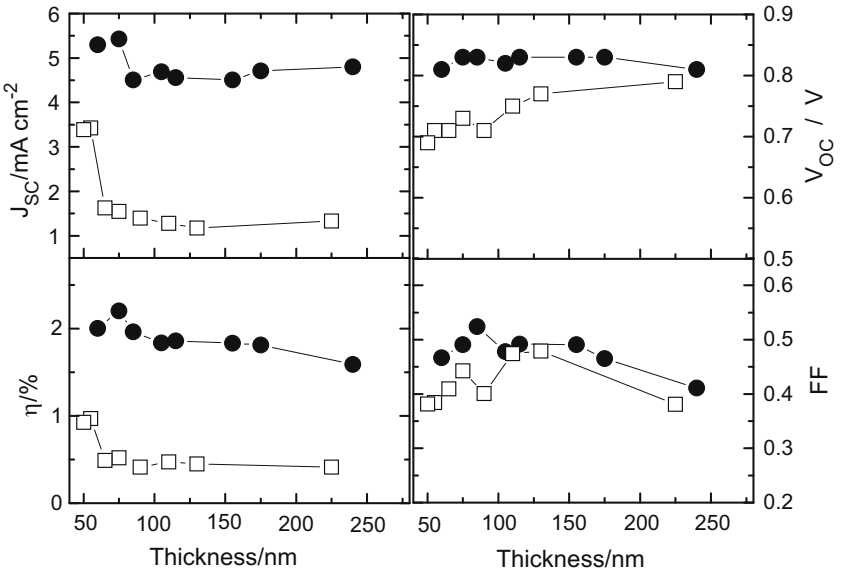


**Fig. 5.** Photovoltaic parameters $V_{OC}$, $J_{SC}$. FF and $\eta$ as a function of active layer thickness for ITO/PEDOT:PSS/PDHeOPV:PCBM (80 wt.% PCBM)/Al (filled squares) and ITO/PEDOT:PSS/MDMO-PPV:PCBM (80 wt.% PCBM)/Al (filled circles) devices.

420–520 nm compared to about 34% for MDMO-PPV:PCBM blend devices.

AFM images show that the surface morphology is different for PDHeOPV:PCBM and for MDMO-PPV:PCBM blend films and that the morphology is affected differently by blend composition in the two cases. For example, phase segregation is observed at 50 wt.% PCBM in PDHeOPV:PCBM blends while none is seen in MDMO-PPV:PCBM until ~67 wt.%. The poorer device performance for PDHeOPV:PCBM than for MDMO-PPV:PCBM can be attributed to the more phase-segregated morphology and poorer transport properties, which in turn limit the thickness of the PDHeOPV:PCBM active layer that can be used for efficient device performance. Furthermore, the strong positive effect of PCBM addition on the hole transport properties observed in MDMO-PPV:PCBM blends was not observed in the case PDHeOPV:PCBM; the mechanism requires further investigation but the different morphology of the blend films is likely to be a factor. Thus it appears that the choice of the symmetric or asymmetric side chains has a clear influence on the blend morphology and transport properties within the blend, and should be taken into consideration in the design of new conjugated polymer materials for photovoltaic applications.

## Acknowledgements

We thank James Kirkpatrick and Panagiotis Keivanidis for helpful discussions. This work was supported by BP Solar (OSCER Project) and the UK Engineering and Physical Sciences Research Council (EP/E036341, Materials for Energy Supply programme).

## References

[1] M. Campoy-Quiles, T. Ferenczi, T. Agostinelli, P.G. Etchegoin, Y. Kim, T.D. Anthopoulos, P.N. Stavrinou, D.D.C. Bradley, J. Nelson, Nature Materials 7 (2008) 158–164.
[2] H. Hoppe, N.S. Sariciftci, Journal of Materials Research 19 (2004) 1924–1945.
[3] J.K.J. van Duren, X.N. Yang, J. Loos, C.W.T. Bulle-Lieuwma, A.B. Sieval, J.C. Hummelen, R.A.J. Janssen, Advanced Functional Materials 14 (2004) 425–434.
[4] J. Peet, J.Y. Kim, N.E. Coates, W.L. Ma, D. Moses, A.J. Heeger, G.C. Bazan, Nature Materials 6 (2007) 497–500.
[5] C. Melzer, E.J. Koop, V.D. Mihailetchi, P.W.M. Blom, Advanced Functional Materials 14 (2004) 865–870.
[6] V.D. Mihailetchi, L.J.A. Koster, P.W.M. Blom, C. Melzer, B. de Boer, J.K.J. van Duren, R.A.J. Janssen, Advanced Functional Materials 15 (2005) 795–801.
[7] C. Muller, T.A.M. Ferenczi, M. Campoy-Quiles, J.V. Frost, D.D.C. Bradley, P. Smith, N. Stingelin-Stutzmann, J. Nelson, Advanced Materials 20 (2008) 3510–3515.
[8] W.J.E. Beek, M.M. Wienk, R.A.J. Janssen, Advanced Functional Materials 16 (2006) 1112–1116.
[9] D. Veldman, O. Ipek, S.C.J. Meskers, J. Sweelssen, M.M. Koetse, S.C. Veenstra, J.M. Kroon, S.S. van Bavel, J. Loos, R.A.J. Janssen, Journal of the American Chemical Society 130 (2008) 7721–7735.
[10] S.E. Shaheen, C.J. Brabec, N.S. Sariciftci, F. Padinger, T. Fromherz, J.C. Hummelen, Applied Physics Letters 78 (2001) 841–843.
[11] C.M. Bjorstrom, K.O. Magnusson, E. Moons, Synthetic Metals 152 (2005) 109–112.
[12] M. Breselge, I. Van Severen, L. Lutsen, P. Adriaensens, J. Manca, D. Vanderzande, T. Cleij, Thin Solid Films 511 (2006) 328–332.
[13] M. Kemerink, J.K.J. van Duren, P. Jonkheijm, W.F. Pasveer, P.M. Koenraad, R.A.J. Janssen, H.W.M. Salemink, J.H. Wolter, Nano Letters 3 (2003) 1191–1196.
[14] V.D. Mihailetchi, J. Wildeman, P.W.M. Blom, Physical Review Letters 94 (2005) 126602–126605.
[15] P.W.M. Blom, V.D. Mihailetchi, L.J.A. Koster, D.E. Markov, Advanced Materials 19 (2007) 1551–1566.
[16] S.M. Tuladhar, M. Sims, J. Kirkpatrick, R.C. Maher, A.J. Chatten, D.D.C. Bradley, J. Nelson, P.G. Etchegoin, C.B. Nielsen, P. Massiot, W.N. George, Joachim H.G. Steinke, Physical Review B 79 (2009) 035201.
[17] T. Kreouzis, D. Poplavskyy, S.M. Tuladhar, M. Campoy-Quiles, J. Nelson, A.J. Campbell, D.D.C. Bradley, Physical Review B 73 (2006).
[18] P.M. Borsenberger, E.H. Magin, M. Vanderauweraer, F.C. Deschryver, Physica Status Solidi A-Applied Research 140 (1993) 9–47.
[19] H. Bassler, Physica Status Solidi B-Basic Research 175 (1993) 15–56.
[20] S.M. Tuladhar, D. Poplavskyy, S.A. Choulis, J.R. Durrant, D.D.C. Bradley, J. Nelson, Advanced Functional Materials 15 (2005) 1171–1182.
[21] T. Fromherz, F. Padinger, D. Gebeyehu, C. Brabec, J.C. Hummelen, N.S. Sariciftci, Solar Energy Materials and Solar Cells 63 (2000) 61–68.
[22] F. Braun, Ph.D.Thesis (2007), University of London, UK.
[23] C.J. Brabec, A. Cravino, D. Meissner, N.S. Sariciftci, M.T. Rispens, L. Sanchez, J.C. Hummelen, T. Fromherz, Thin Solid Films 403 (2002) 368–372.
[24] V.D. Mihailetchi, P.W.M. Blom, J.C. Hummelen, M.T. Rispens, Journal of Applied Physics 94 (2003) 6849–6854.